

7-2012

# A Model for Blue Crab Population in the Chesapeake Bay

Timothy J. Becker  
*College of William and Mary*

Follow this and additional works at: <http://publish.wm.edu/honorsthesis>

---

## Recommended Citation

Becker, Timothy J., "A Model for Blue Crab Population in the Chesapeake Bay" (2012). *Undergraduate Honors Theses*. Paper 495.  
<http://publish.wm.edu/honorsthesis/495>

This Honors Thesis is brought to you for free and open access by the Theses, Dissertations, & Master Projects at W&M Publish. It has been accepted for inclusion in Undergraduate Honors Theses by an authorized administrator of W&M Publish. For more information, please contact [wpublish@wm.edu](mailto:wpublish@wm.edu).

**A Model for Blue Crab Population  
in the Chesapeake Bay**

A thesis submitted in partial fulfillment of the requirement  
for the degree of Bachelors of Science in Mathematics from  
The College of William and Mary

by

Timothy J. Becker

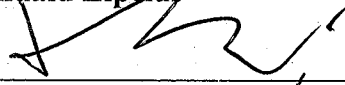
Accepted for honors



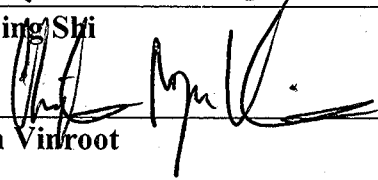
Leah Shaw, Director



Romuald Lipcius



Junping Shi



Ryan Vinroot

Williamsburg, VA  
May 1, 2012

A Model for the Population  
of the Blue Crab in the Chesapeake Bay

Timothy J. Becker

Department of Mathematics,  
College of William and Mary,  
Williamsburg, VA 23187-8795, USA

Email: [tjbecker@email.wm.edu](mailto:tjbecker@email.wm.edu)

May 10, 2012

## **Abstract**

We model the population of the Blue Crab in the Chesapeake Bay by using differential equations. Blue crabs are inherently cannibalistic of juveniles, while also in competition with juvenile blue crabs for resources. These differential equations describe the intraguild predation consistent in the blue crab food web, as well as the cannibalistic nature of the blue crab. We introduce an aging and birth rate to alter an intraguild predation model to fit the cannibalistic nature.

# Contents

<b>1</b>	<b>Introduction</b>	<b>1</b>
1.1	Background on Blue Crab . . . . .	1
1.2	Basic Ecological Interactions . . . . .	2
1.3	Review of models of Intraguild Predation and Cannibalism . . . . .	4
1.4	Summary of Results . . . . .	7
<b>2</b>	<b>Mathematical Model</b>	<b>9</b>
2.1	Model Setup . . . . .	9
2.2	Parameter Estimates . . . . .	12
2.3	Non-dimensionalization . . . . .	14
<b>3</b>	<b>Analysis and Simulation of the Model</b>	<b>17</b>
3.1	Stability Analysis . . . . .	18
3.2	Lotka-Volterra Case . . . . .	22
3.2.1	Lotka-Volterra Bifurcation Derivative . . . . .	24
3.3	Holling Type II Case . . . . .	25
3.3.1	Holling Type II Bifurcation Derivative . . . . .	26
3.4	Numerical Simulations . . . . .	28
3.4.1	Matlab Code for Numerical Simulations . . . . .	33
<b>4</b>	<b>Conclusions</b>	<b>35</b>

4.1 Acknowledgements . . . . .	37
--------------------------------	----

# List of Figures

1.1	Blue Crab Food Web (from [13]) . . . . .	3
2.1	Flow Diagram. See text for details. . . . .	11
3.1	Bifurcation Diagram of Lotka-Volterra Case (3.28) . . . . .	24
3.2	Bifurcation Diagram with Bistability of Lotka-Volterra Case (3.28) . . . . .	25
3.3	Bifurcation Diagram of (3.35) . . . . .	26
3.4	Bifurcation Diagram with Bistability of (3.35) . . . . .	28
3.5	Extinction of Resource: $\nu_1 > \tilde{\nu}_1$ . The solution approaches $(0, V^*, W^*)$ . . . . .	30
3.6	Persistence of Blue Crab: $\nu_1^* < \nu_1 < \tilde{\nu}_1$ . The solution approaches $(U^*, V^*, W^*)$ 31	
3.7	Extinction of Blue Crab: $\nu_1 < \nu_1^*$ . The solution approaches $(\kappa, 0, 0)$ . . . . .	32





# Chapter 1

## Introduction

### 1.1 Background on Blue Crab

The blue crab (*Callinectes Sapidus*) is an aquatic organism which plays a large role in the food chain in the Chesapeake Bay. Additionally, the blue crab is the highest grossing of any of the commercial fisheries in the Chesapeake Bay and makes up approximately one third of the nation's catch of blue crab. The population of the blue crab in the Chesapeake Bay has been well below its historic level, which is one of the driving factors of this study. In 2009, the adult blue crab population reached above 200 million for the first time since 1993. The population of the juveniles, however, is still well below the historic average.

The blue crab partakes in intraguild predation, which is a subset of omnivory. Omnivory is commonly defined as predation over more than one trophic level [11]. In this case, we have the blue crab, which eats both juvenile blue crabs as well as the bivalves that juvenile blue crabs eat[13, pg. 592]. Thus, the blue crab is a predator who eats over more than one trophic level. Omnivory such as this was thought to be quite rare in food webs, but now it has been found to be very common[15]. Even further, omnivory can act as a local stabilizer in food webs[15]. As such, it is not unexpected that the blue crab partakes in a food web that contains omnivory.

To make a model of the blue crab population with intraguild predation and cannibalism present, we must have a distinct break between juvenile and adult for the blue crab population, based on either age or size. The juvenile blue crabs are put into size classes based on their carapace width (CW). Cannibalism becomes apparent in juvenile blue crabs when they reach a size of  $\geq 40$  mm CW [13, pg. 547]. However, it is not until juveniles reach a size of  $\geq 60$  mm CW that other blue crabs make up a significant portion of their diet [13, pg. 548]. This is around the 7th-9th instar, still less than one year old [13, pg. 546]. Blue crabs specifically cannibalize intermolt juvenile blue crabs [13, pg. 621]. As such, there is a disparity between when blue crabs become sexually mature, around 12 – 18 months, and when blue crabs start to cannibalize younger blue crabs [13]. Taking all of this into account, we will conclude for the sake of this model that juveniles are up to one year in age, and adults are one year and older.

The diet for the blue crab is important to this study so as to accurately determine the population dynamics of the resource, for which the juvenile and adult blue crab will compete. Adult blue crabs consume over 99 species, mainly mollusks (20–40% of stomach content), arthropods (10 – 26%), chordates (5 – 12%), and annelids (1 – 7%), along with juvenile blue crabs [13, pg. 592]. Juvenile blue crabs mainly feed on bivalves, crustaceans, and detritus, or plant matter [13, pg. 548]. Figure 1.1 shows the more detailed food web, with darker lines showing a stronger predation. From this, we can say for this study that the resource could be considered to be from the mollusk phylum, with a specific point of emphasis on bivalves.

## 1.2 Basic Ecological Interactions

There are different types of interaction that can occur between species in nature. We will focus on the two types that are prevalent to our model. The first is a Predator-Prey relationship, while the second is Competition. These two types of interaction are the foundations of complex food webs [11]. We do not focus on commensalism, mutualism,

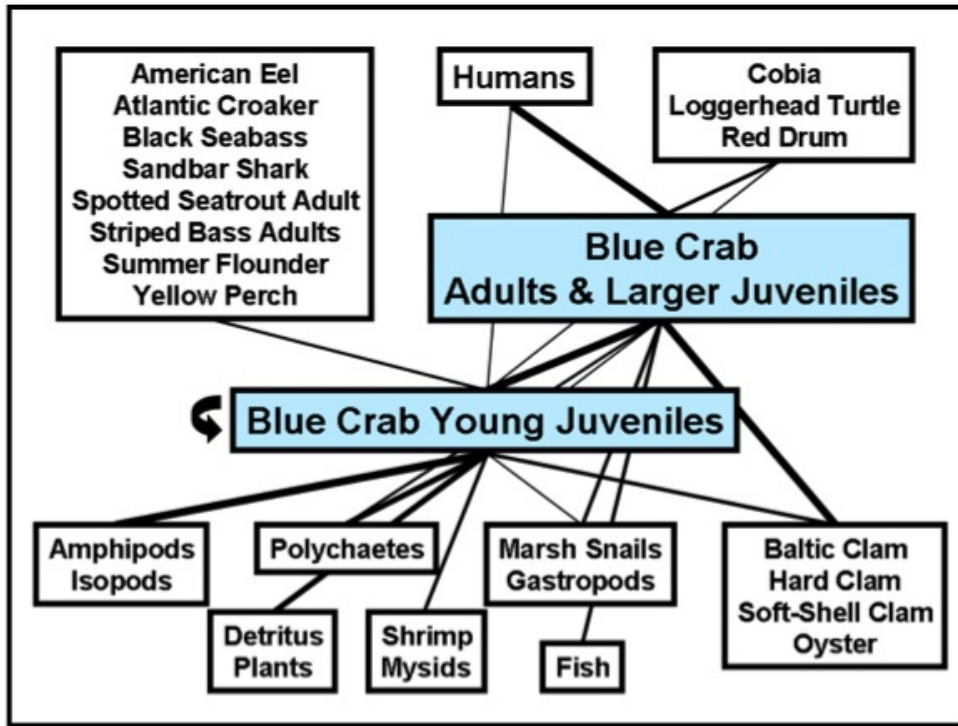


Figure 1.1: Blue Crab Food Web (from [13])

or amensalism here, since none are prevalent in our model [16].

The Predator-Prey relationship is one that spans two different trophic levels. The predator is at one trophic level, and the prey is at a lower trophic level. The Lotka-Volterra model was one of the first models to incorporate the predator-prey relationship [12, 21].

We have three types of functional responses that we can study as well. These describe the organism's capacity to catch, eat, and process their prey. They are the predation rate per prey as a function of the number of predators. There is the linear (Lotka-Volterra) case, as well as the more complicated Holling Type II and Holling Type III cases [20].

The linear case describes a predator that eats whenever it comes into contact with prey and never becomes satiated. As such, we have a simple term for predation  $aNP$ . This term consists of a constant predation rate  $a$  and then multiplied by the population

of the prey,  $N$ , and the predator  $P$ .

The Holling Type II Functional Response describes a predator who eats until it is full, then processes the food, then searches for more food. Thus, we use a term that describes this behavior, namely  $\frac{aNP}{ahN + 1}$ . This term consists of the same linear case in the numerator, but also with a function in the denominator that demonstrates the capacity of the predator to become “full” based on the amount of resource available to consume [17]. The parameter  $h$  is the handling time, which is the amount of time needed to catch, eat, and process the prey.

The Holling Type III Functional Response, which we do not use in our model, is a sigmoidal function that describes the same phenomenon of saturation of a predator at high-density levels of the prey, but also is more than just a linear relationship at low density of the prey. It is in a form  $\frac{aN^2P}{ahN^2 + 1}$ . This describes the “learning” of the predator [17].

### 1.3 Review of models of Intraguild Predation and Cannibalism

Intraguild predation is a subset of omnivory, in which two species at different trophic levels compete for prey at a lower trophic level, where a trophic level is defined as the organism’s position in the food chain [16]. Intraguild predation can be defined as the predation of a prey species by a predator that also preys on the resource of the prey[11]. Thus, both the predator and the prey are competitors for the resource in question, which adds a new dimension into the food web. The act of predation by the predator on the prey reduces the potential for competition for the resource[16]. Intraguild predation can also promote alternative stable states, depending on the situation[16]. Systems containing intraguild predation can produce a variety of these alternative states, as well as behaviors [11].

One of the earliest models of intraguild predation was done by Holt and Polis [11],

and their model is in the following form:

$$\begin{aligned}
\frac{dR}{dt} &= R[\phi(R) - a(R, N, P)N - a'(R, N, P)P], \\
\frac{dN}{dt} &= N[ba(R, N, P)R - \alpha(R, N, P)P - m], \\
\frac{dP}{dt} &= P[b'a'(R, N, P)R + \beta\alpha(R, N, P)N - m'],
\end{aligned} \tag{1.1}$$

where  $R$  is the resource,  $N$  is the intraguild prey, and  $P$  is the intraguild predator [11]. The resource growth rate per capita is  $\phi(R)$ , while  $b, b'$ , and  $\beta$  are rates of efficiency of the predation. The functions  $a(R, N, P)$ ,  $a'(R, N, P)$ , and  $\alpha(R, N, P)$  are the predation terms. The mortality rates are  $m$  and  $m'$  for the intraguild prey and predator, respectively. This model can be simplified to a standard Lotka-Volterra model with intraguild predation inserted into it. To make such a model, we set  $a, a'$ , and  $\alpha$  as constants, as well as taking  $\phi(R) = 1 - \frac{R}{K}$ , describing logistic growth [11]. The logistic growth describes the growth of the resource, beginning exponentially, but then slowing as the saturation begins, until stopping completely at a carrying capacity,  $K$ . We will use logistic growth for the resource in our model in Chapter 2. The simplified model is as follows:

$$\begin{aligned}
\frac{dR}{dt} &= R \left[ r \left( 1 - \frac{R}{K} \right) - aN - a'P \right], \\
\frac{dN}{dt} &= N(abR - m - \alpha P), \\
\frac{dP}{dt} &= P(b'a'R + \beta\alpha N - m').
\end{aligned} \tag{1.2}$$

We can also let  $a, a'$ , and  $\alpha$  be set as Holling Type II functional responses. One of the newest models of intraguild predation is that of Verdy and Amarasekere, which uses Holling Type II functional responses [20]. This model has built upon Holt and Polis'

previous model. Verdy and Amarasekere's intraguild predation model is as follows[20]:

$$\begin{aligned}\frac{dR}{dt} &= S(R) + I - E(R) - \frac{aR}{x_1}N - \frac{a'R}{x_2}P, \\ \frac{dN}{dt} &= \frac{baR}{x_1}N - \frac{\alpha N}{x_2}P - mN, \\ \frac{dP}{dt} &= \frac{b'a'R}{x_2}P + \frac{\beta\alpha N}{x_2}P - m'P,\end{aligned}\tag{1.3}$$

where

$$x_1 = ahR + 1, \quad \text{and} \quad x_2 = a'h'R + \alpha\eta N + 1;$$

and

$$S(R) = rR \left(1 - \frac{R}{K}\right), \quad I = \rho\chi \quad \text{and} \quad E(R) = \tilde{\rho}R.$$

Here  $R$  is the resource,  $N$  is the prey, and  $P$  is the predator. The resource modeled from the logistic growth ( $S(R)$ ), immigration ( $I$ ), emigration ( $E(R)$ ), and interaction between the resource and both the prey and the predator. The rate of consumption of the resource by the prey is  $a$ , with a handling time  $h$ , and  $b$  is the efficiency [20]. In the same manner,  $a'$  is the rate of consumption of the resource by the predator, with handling time  $h'$  and efficiency  $b'$ , and  $\alpha$  is the rate of consumption of the prey by the predator, with handling time  $\eta$  and efficiency  $\beta$  [20]. The rates of supply and loss for the resource are  $\rho$  and  $\tilde{\rho}$ , and  $\chi$  is the input resource concentration [20]. The maximum growth rate per capita is  $r$ , while  $K$  is the carrying capacity [20]. The rate of mortality of the prey is  $m$  and  $m'$  is the rate of mortality of the predator [20].

In accordance with intraguild predation, the blue crab is inherently cannibalistic[13](pg. 620). Thus, in terms of intraguild predation, the predator is the blue crab adult, while the prey is the blue crab juvenile. Cannibalism can be a regulator of population density and an equilibrator, while it can also result in oscillations in the population density, depending on the situations within which the cannibalism is inherent[8]. Cannibalism can, additionally, help a population survive. The lifeboat strategy declares that what the species gains from cannibalism in times of scarcity in other resources can keep a species from going extinct when it would otherwise[8]. Cannibalism has inherently negative and

positive feedbacks which lead to many different steady states and hysteresis effects, which is a system that has “memory” [8].

## 1.4 Summary of Results

We will construct a model based on the intraguild predation model of Verdy and Amasekere discussed in Section 1.3. Our model describes the intraguild predation within the blue crab food web as well as the cannibalism that takes place on juvenile blue crabs by adult blue crabs. Analysis shows that we have a trivial and semi-trivial equilibrium, as well as a stable co-existence equilibrium. Bifurcation analysis shows that the blue crab model demonstrates the possibility of bistability in the system. As a caveat, we recognize that our parameter estimates are good, but not exact, and we believe that this contributes to results such as the stability of the unreasonable equilibrium that was found.





# Chapter 2

## Mathematical Model

### 2.1 Model Setup

We build our model based on Verdy and Amarasekere's model in Equation (1.3). Firstly, however, we are modeling our populations in biomass, as opposed to numbers of individuals. We can start thinking of the predator as the cannibalistic adult, and the prey as the juvenile, as well as bivalves for the resource [13]. We introduce an aging term,  $eN$  into the intraguild predation model, to give this model some semblance of a model with both intraguild predation and cannibalism. We introduced a Beverton-Holt birth term into the differential equation for our juveniles, which depends on the population of the adults. This is because reproduction by the predator will increase the population of the prey, not of the predator itself. This birth term is the only increase in the model due to reproduction. Every other positive term is growth of biomass for the species, due to predation or aging. Additionally, we removed the reproduction term for the juvenile based on predation of the bivalves because the juveniles are unable to reproduce. We also assume the immigration and emigration  $I = E(R) = 0$  as the population in the bay is essentially closed to the outside. Additionally, we substitute in for  $x_1, x_2$ , and  $S(R)$  from the definitions of these parameters [20]. We also replace  $\alpha$  with  $a''$  and  $\eta$  with  $h''$ . So, we

have:

$$\begin{aligned}
\frac{dR}{dt} &= rR \left(1 - \frac{R}{k}\right) - \frac{aRN}{ahR + 1} - \frac{a'RP}{a'h'R + a''h''N + 1}, \\
\frac{dN}{dt} &= \frac{nP}{1 + n'P} + \frac{baRN}{ahR + 1} - eN - mN - \frac{a''NP}{a'h'R + a''h''N + 1}, \\
\frac{dP}{dt} &= eN + \frac{b'a'RP}{a'h'R + a''h''N + 1} + \frac{b''a''NP}{a'h'R + a''h''N + 1} - m'P - fP,
\end{aligned} \tag{2.1}$$

Thus, we have an intraguild predation model that includes the population of the juvenile depending on the birth rate of the adult and both the adult and juvenile depend on the aging rate of the juvenile. Tables 2.1 and 2.2 describe the specific parameters and their values, so here we will describe what each term demonstrates. The equation for the resource  $R(t)$  consists of the logistic term is  $rR \left(1 - \frac{R}{K}\right)$ , the term describing consumption of the resource by the juvenile is  $\frac{aRN}{ahR + 1}$ , and the term describing consumption of the resource by the cannibalistic adults is  $\frac{a'RP}{a'h'R + a''h''N + 1}$ . Both food sources are described in the denominator here to show that if  $R$  goes to infinity, then this predation becomes linear in predator density, due to the amount of resource available. If  $N$  goes to infinity, however, consumption of resource by adults will go to 0 due to the increase in predation on the prey.

Similarly, we can study the equation for the juvenile population  $N(t)$ . The equation for the juveniles consists of the Beverton-Holt birth term is  $\frac{nP}{1 + n'P}$ . The term describing consumption of the resource by the prey is  $\frac{b'a'RP}{a'h'R + a''h''N + 1}$ , and the term describing the aging rate of juveniles into adults is  $eN$ . Lastly, we have the term for intrinsic mortality rate of juveniles as  $mN$ , and the term representing the predation of the juvenile by the cannibalistic adult is  $\frac{a''NP}{a'h'R + a''h''N + 1}$ . This contains both food sources in the denominator as well, for the same reasons as the adult predation on the resource.

The equation for the cannibalistic adults  $P(t)$  also includes the term representing the aging of juveniles into adults:  $eN$ , except it is positive here. The term for the consumption of the bivalves by the adults is  $\frac{b'a'RP}{a'h'R + a''h''N + 1}$ , and the cannibalistic

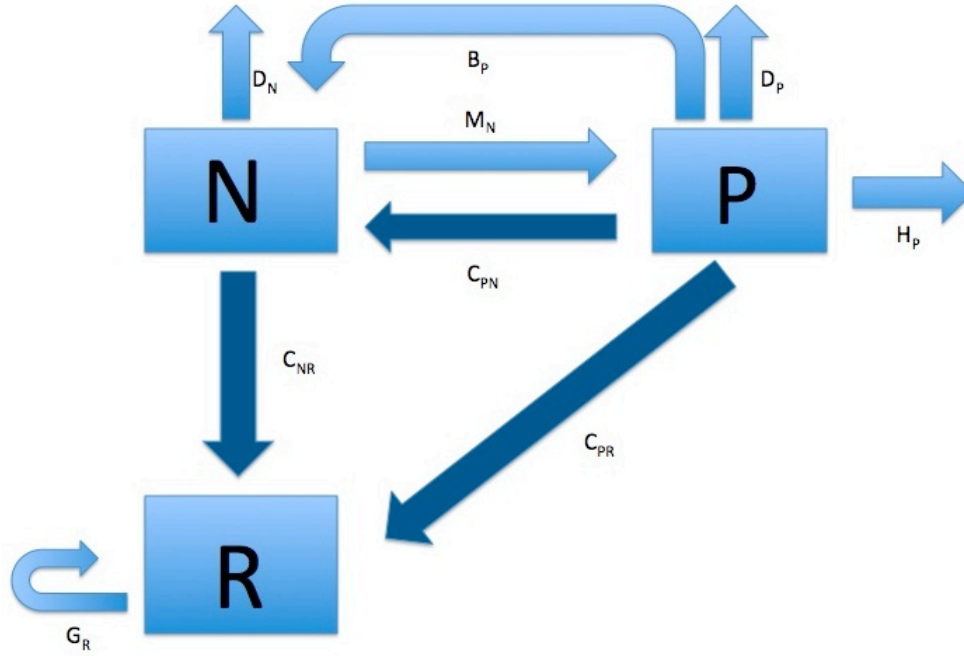


Figure 2.1: Flow Diagram. See text for details.

term for the consumption of the juveniles is  $\frac{b''a''NP}{a'h'R + a''h''N + 1}$ . Lastly, we define the losses from intrinsic mortality as  $m'P$  and from harvesting as  $fP$ .

The flow diagram in Fig. 2.1 describes graphically the interactions between the bivalves, juvenile blue crabs, and adult blue crabs. In the diagram,  $G_R$  is the growth of the resource,  $C_{NR}$ ,  $C_{PR}$  and  $C_{PN}$  are the consumption of resource by the juvenile, the adult, and the consumption of the juvenile by the adult respectively,  $D_N$  and  $D_P$  are the death of the juvenile and adult,  $M_N$  and  $B_P$  are the aging and new birth, respectively, between the juvenile and adult, and  $H_P$  is the harvesting of the adult. Each of  $M_N$ ,  $C_{NR}$ ,  $C_{PR}$  and  $C_{PN}$  represent two terms (gain and loss) in the system of equations, and each of other arrows represents one term.

## 2.2 Parameter Estimates

We define our time in years and our population of organisms in kilograms of biomass per square meter in the Chesapeake Bay.

<i>Variables</i>	<i>Meaning</i>	<i>Dimension</i>	<i>Units</i>
$t$	Time	$T$	years
$R(t)$	Bivalves	$A$	kg biomass/ $m^2$
$N(t)$	Juvenile Blue Crabs	$B$	kg biomass/ $m^2$
$P(t)$	Adult Blue Crabs	$B$	kg biomass/ $m^2$

Table 2.1: Model variables in (2.1). Dimension A is kg of resource biomass per square meter, Dimension B is kg of blue crab biomass per square meter

We find the predation rates of the adult blue crab in Eggleston [9, *TableIV*], using the values for  $a'$  in their paper and converting to our model. From here, we then scale our new value for our own  $a'$  using the metabolic scaling rate to find the predation rate of the juvenile blue crab. We assume that predation rate is proportional to metabolic rate, so we used the allometric scaling model [6]:

$$Y = Y_0 M^{3/4}, \quad (2.2)$$

for  $M$  being the mass of the organism,  $Y$  a dependent variable, which we take as metabolic rate, and  $Y_0$  as an unknown constant of proportionality. The handling rates,  $h$ ,  $h'$ , and  $h''$  are determined using  $T_h$  [9, *TableIV*].

For the mortality rate of the adult,  $m'$ , as well as the mortality due to fishing,  $f$ , we use the Stock Assessment of the Blue Crab in the Chesapeake Bay from 2011 [19]. The resource growth rate,  $r$ , the carrying capacity,  $k$ , and the juvenile mortality rate,  $m$ , come from conversation with the researchers at the Virginia Institute of Marine Science [18].

All the parameters are summarized in Table 2.2.

	<i>Meaning</i>	<i>Dimension</i>	<i>Value</i>	<i>Source</i>
$r$	Resource Growth Rate	$T^{-1}$	0.5	[18]
$k$	Carrying Capacity	$A$	0.2	[18]
$a$	Rate of Consumption of the Resource by the Juveniles	$T^{-1}B^{-1}$	0.43	[9]
$h$	Handling Time of the Juveniles for Resource Consumption	$TBA^{-1}$	0.1	[9]
$a'$	Rate of Consumption of the Resource by the Adults	$T^{-1}B^{-1}$	1.44	[9]
$h'$	Handling Time of the Adults for Resource Consumption	$TBA^{-1}$	0.1	[9]
$a''$	Rate of Consumption of the Juveniles by the Adults	$T^{-1}B^{-1}$	1.44	[9]
$h''$	Handling Time of the Adults for Juvenile Consumption	$T$	0.1	[9]
$m$	Natural Mortality Rate of the Juveniles	$T^{-1}$	1.5	[18]
$e$	Aging Rate of the Juveniles	$T^{-1}$	1	[18]
$b$	Rate of Efficiency of Resource Consumption by Juveniles	$BA^{-1}$	0.1	[9]
$b'$	Rate of Efficiency of Resource Consumption by Adults	$BA^{-1}$	0.1	[9]
$b''$	Rate of Efficiency of Juvenile Consumption by Adults	1	0.1	[9]
$m'$	Natural Mortality Rate of the Adults	$T^{-1}$	0.9	[19]
$f$	Fishing Mortality	$T^{-1}$	0.7	[19]
$n$	Proliferation Rate	$T^{-1}$	1	[18]
$n'$	Saturation Rate	$B^{-1}$	1	[18]

Table 2.2: Original Parameters in (2.1)

## 2.3 Non-dimensionalization

We use the following change of parameters to non-dimensionalize the system:

$$s = rt, \quad U = ahR, \quad V = \frac{N}{b'k}, \quad W = \frac{P}{khr}. \quad (2.3)$$

Our new dimensionless model is as follows:

$$\begin{aligned} \frac{dU}{ds} &= U \left( 1 - \frac{U}{\kappa} \right) - \frac{\gamma_1 UV}{U+1} - \frac{\lambda_1 UW}{\theta U + \delta \psi V + 1}, \\ \frac{dV}{ds} &= \frac{\nu_1 W}{1 + \nu_2 W} + \frac{\gamma_2 UV}{U+1} - \mu_1 V - \frac{\delta VW}{\theta U + \delta \psi V + 1}, \\ \frac{dW}{ds} &= \epsilon V - \mu_2 W + \frac{\gamma_3 UW + \delta \gamma_4 VW}{\theta U + \delta \psi V + 1}, \end{aligned} \quad (2.4)$$

where the new dimensionless parameters are:

$$\begin{aligned} \kappa &= ahk, \quad \gamma_1 = \frac{ab'k}{r}, \quad \lambda_1 = a'hk, \quad \theta = \frac{a'h'}{ah}, \\ \psi &= \frac{h''b'}{h}, \quad \nu_1 = \frac{nh}{b}, \quad \nu_2 = n'khr, \quad \gamma_2 = \frac{b}{hr}, \quad \delta = a''hk, \\ \mu_1 &= \frac{m+e}{r}, \quad \epsilon = \frac{eb'}{hr^2}, \quad \gamma_3 = \frac{a'b'}{ahr}, \quad \mu_2 = \frac{m'+f}{r}, \quad \gamma_4 = \frac{b'b''}{hr}. \end{aligned} \quad (2.5)$$

The majority of the new parameters are rescaling of the old parameters, although we do have  $r$  becoming 1 and  $m_2$  and  $f$  being combined into  $\mu_2$ . All the new parameters in (2.4) are summarized in Table 2.3, and the parameter values are converted from Table 2.2 and (2.5). In the following chapters, we will analyze this dimensionless model (2.4).

	<i>Meaning</i>	<i>Value</i>
$\kappa$	Carrying Capacity	0.0086
$\gamma_1$	Rate of Consumption of the Resource by the Juveniles	0.0172
$\gamma_2$	Rate of Efficiency of Resource Consumption by Juveniles	2
$\gamma_3$	Rate of Efficiency of Resource Consumption by Adults	6.6977
$\gamma_4$	Rate of Efficiency of Juvenile Consumption by Adults	0.2
$\lambda_1$	Rate of Consumption of the Resource by the Adults	0.0288
$\theta$	Ratio of Adult and Juvenile Predation of Resource	3.3488
$\psi$	Ratio of Handling Times	0.01
$\nu_1$	Proliferation Rate of Blue Crabs	1
$\nu_2$	Saturation Rate of Crab Proliferation	0.1
$\delta$	Rate of Consumption of the Juveniles by the Adults	0.0288
$\mu_1$	Mortality Rate of the Juveniles	5
$\mu_2$	Mortality Rate of the Adults	3.2
$\epsilon$	Aging Rate of the Juveniles	4

Table 2.3: New Parameters in (2.4)





# Chapter 3

## Analysis and Simulation of the Model

In order to incorporate both Lotka-Volterra and Holling Type II functional responses, we consider a system of equations in a more general form:

$$\begin{aligned}\frac{dU}{ds} &= U\phi(U) - a_1(U)UV - a_2(U, V)UW, \\ \frac{dV}{ds} &= \frac{\nu_1 W}{1 + \nu_2 W} + b_1 a_1(U)UV - \mu_1 V - b_2 a_2(U, V)VW, \\ \frac{dW}{ds} &= \epsilon V - \mu_2 W + b_3 a_2(U, V)UW + b_4 a_2(U, V)VW,\end{aligned}\tag{3.1}$$

where all parameters are the same as in Chapter 2,  $\phi(U) = 1 - \frac{U}{\kappa}$  is the logistic growth of the bivalves, and  $a_1(U)$  and  $a_2(U, V)$  are predation rates.

We will consider two cases. Firstly, we have the Lotka-Volterra case, in which

$$a_1(U) = a_1 = \gamma_1, \quad \text{and} \quad a_2(U, V) = a_2 = \lambda_1.\tag{3.2}$$

Secondly, we have the Holling Type II case, where

$$a_1(U) = \frac{\gamma_1}{U + 1}, \quad a_2(U, V) = \frac{\lambda_1}{\theta U + \delta \psi V + 1},\tag{3.3}$$

and additionally we have the following new parameters:

$$b_1 = \frac{\gamma_2}{\gamma_1}, \quad b_2 = \frac{\delta}{\lambda_1}, \quad b_3 = \frac{\gamma_3}{\lambda_1}, \quad b_4 = b_2\gamma_4. \quad (3.4)$$

With the definitions in (3.3) and (3.4), the general system (3.1) includes (2.4) as a special case.

For (3.1), there is the trivial equilibrium  $(0, 0, 0)$  as well as the semi-trivial equilibria  $(\kappa, 0, 0)$  and  $(0, V^*, W^*)$ . We will do the stability analysis for these three equilibria in the general situation and then we will apply it to the two specific cases.

### 3.1 Stability Analysis

The stability of the equilibria is determined by the Jacobian matrix. If all of the eigenvalues have negative real parts, then the equilibrium is stable. Otherwise, the equilibrium is unstable. When certain parameters change, the stability of the equilibrium changes from stable to unstable or vice versa, then a bifurcation could occur.

We linearize the system (3.1) and find the Jacobian to be:

$$J(U, V, W) = \begin{pmatrix} J_{11} & J_{12} & J_{13} \\ J_{21} & J_{22} & J_{23} \\ J_{31} & J_{32} & J_{33} \end{pmatrix}. \quad (3.5)$$

where

$$J_{11} = U\phi'(U) + \phi(U) - a_1(U)V - a_1'(U)UV - \frac{\partial a_2}{\partial U}UW - a_2(U, V)W, \quad (3.6)$$

$$J_{12} = -a_1(U)U - \frac{\partial a_2}{\partial V}UW, \quad (3.7)$$

$$J_{13} = -a_2(U, V)U, \quad (3.8)$$

$$J_{21} = b_1a_1'(U)UV + b_1a_1(U)V - b_2\frac{\partial a_2}{\partial U}VW \quad (3.9)$$

$$J_{22} = b_1a_1(U)U - \mu_1 - b_2\frac{\partial a_2}{\partial V}VW - b_2a_2(U, V)W \quad (3.10)$$

$$J_{23} = \frac{\nu_1}{(1 + \nu_2 W)^2} - b_2 a_2(U, V) V \quad (3.11)$$

$$J_{31} = b_3 \frac{\partial a_2}{\partial U} U W + b_3 a_2(U, V) W + b_4 \frac{\partial a_2}{\partial U} V W \quad (3.12)$$

$$J_{32} = \epsilon + b_3 \frac{\partial a_2}{\partial V} U W + b_4 \frac{\partial a_2}{\partial V} V W + b_4 a_2(U, V) W \quad (3.13)$$

$$J_{33} = -\mu_2 + b_3 a_2(U, V) U + b_4 a_2(U, V) V. \quad (3.14)$$

For the  $(0, 0, 0)$  equilibrium, the Jacobian becomes:

$$J(0, 0, 0) = \begin{pmatrix} \phi(0) & 0 & 0 \\ 0 & -\mu_1 & \nu_1 \\ 0 & \epsilon & -\mu_2 \end{pmatrix}. \quad (3.15)$$

Define the eigenvalues of  $J(0, 0, 0)$  to be  $\Lambda_1, \Lambda_2$ , and  $\Lambda_3$ . Then  $\Lambda_1 = \phi(0) = 1$  and  $\Lambda_2$  and  $\Lambda_3$  are determined by the characteristic equation for the lower right  $2 \times 2$  block matrix:

$$\Lambda^2 + (\mu_1 + \mu_2)\Lambda + \mu_1\mu_2 - \nu_1\epsilon = 0. \quad (3.16)$$

Since we have at least one positive eigenvalue, we see that the  $(0, 0, 0)$  equilibrium is unstable for both the Lotka-Volterra case and the Holling Type II case. An additional positive eigenvalue may arise if  $\mu_1\mu_2 - \nu_1\epsilon < 0$ . By using  $\nu_1$  as our bifurcation parameter, there is only one positive eigenvalue  $\Lambda_1$  when  $\nu_1 < \nu_1^\#$ , and there are two positive eigenvalues when  $\nu_1 > \nu_1^\#$ , where

$$\nu_1^\# = \frac{\mu_1\mu_2}{\epsilon}. \quad (3.17)$$

This  $\nu_1^\#$  is a bifurcation point at which a branch of semitrivial solutions  $(0, V^*, W^*)$  bifurcates from the unstable trivial equilibrium  $(0, 0, 0)$ .

For the  $(\kappa, 0, 0)$  equilibrium, the Jacobian is:

$$J(\kappa, 0, 0) = \begin{pmatrix} \kappa\phi'(\kappa) & -a_1(\kappa)\kappa & -a_2(\kappa, 0)\kappa \\ 0 & b_1 a_1(\kappa)\kappa - \mu_1 & \nu_1 \\ 0 & \epsilon & -\mu_2 + b_3 a_2(\kappa, 0)\kappa \end{pmatrix}. \quad (3.18)$$

Define the eigenvalues of  $J(\kappa, 0, 0)$  to be  $\Lambda'_1 = -1$  and  $\Lambda'_2$  and  $\Lambda'_3$  are determined by the trace and determinant of the characteristic equation of the lower right  $2 \times 2$  block matrix.

We have:

$$Tr(J(\kappa, 0, 0)) = b_1 a_1(\kappa) \kappa + b_3 a_2(\kappa, 0) \kappa - \mu_1 - \mu_2, \quad (3.19)$$

$$Det(J(\kappa, 0, 0)) = (b_1 a_1(\kappa) \kappa - \mu_1)(-\mu_2 + b_3 a_2(\kappa, 0) \kappa) - \nu_1 \epsilon. \quad (3.20)$$

For the equilibrium to be stable, we need  $Tr(J(\kappa, 0, 0)) < 0$  and  $Det(J(\kappa, 0, 0)) > 0$ . Thus, using  $\nu_1$ , which is our proliferation rate of the blue crabs, as a bifurcation parameter, we see that the semi-trivial equilibrium  $(\kappa, 0, 0)$  is locally stable when  $\nu_1 < \nu_1^*$ , and is unstable when  $\nu_1 > \nu_1^*$ , where

$$\nu_1^* = \frac{(\mu_1 - b_1 a_1(\kappa) \kappa)(\mu_2 - b_3 a_2(\kappa, 0) \kappa)}{\epsilon}. \quad (3.21)$$

This is the bifurcation parameter at which the positive solution  $(U^*, V^*, W^*)$  bifurcates from  $(\kappa, 0, 0)$ .

For future reference, for a possible  $(0, V^*, W^*)$  equilibrium, we have:

$$J(0, V^*, W^*) = \begin{pmatrix} \phi(0) - a_1(0)V^* - a_2(0, V^*)W^* & 0 & 0 \\ b_1 a_2(0, V^*)V^* - b_2 \frac{\partial a_2}{\partial U} V^* W^* & -\mu_1 - b_2 \frac{\partial a_2}{\partial U} V^* W^* - a_2(0, V^*)W^* & \frac{\nu_1}{(1 + \nu_2 W^*)^2} - a_2(0, V^*)V^* \\ b_3 a_2(0, V^*)W^* + b_4 \frac{\partial a_2}{\partial U} V^* W^* & \epsilon + b_4 \frac{\partial a_2}{\partial V^*} V^* W^* + b_2 a_2(0, V^*)W^* & b_4 a_2(0, V^*)V^* - \mu_2 \end{pmatrix}. \quad (3.22)$$

At each of the bifurcation values  $\nu_1 = \nu_1^*$  and  $\nu_1 = \nu_1^\#$ , a transcritical bifurcation occurs. To study the details of the transcritical bifurcation, we use a theorem that allows us to find the direction of the bifurcating curve (a derivative at the bifurcation point), which will determine whether the system has evidence of bistability [7] (here we only state a special case).

In the following theorem,  $N$  is the kernel space,  $R$  is the range space,  $u \in \mathbf{R}^n$ ,  $F_u$  is the partial derivative of  $F$  with respect to  $u$ , and  $F_{\nu_1, u}$  is the second order mixed partial derivative of  $F$  with respect to  $\nu_1$  and  $u$ . The dot product in  $\mathbf{R}^n$  space is  $\langle l, y \rangle$  for  $l, y \in \mathbf{R}^n$ .

**Theorem 3.1.** *Let  $F : \mathbf{R} \times U \rightarrow \mathbf{R}^n$  be twice continuously differentiable, where  $U$  is an open subset of  $\mathbf{R}^n$ . Suppose that  $F(\nu_1, u_0) = 0$  for  $\nu_1 \in \mathbf{R}$ , and at  $(\nu_{1_0}, u_0)$ ,  $F$  satisfies*

**(F1)**  $\dim N(F_u(\nu_{1_0}, u_0)) = \text{codim} R(F_u(\nu_{1_0}, u_0)) = 1$ , and  $N(F_u(\nu_{1_0}, u_0)) = \text{Span}\{w_0\}$ ;

**(F3)**  $F_{\nu_1 u}(\nu_{1_0}, u_0)[w_0] \notin R(F_u(\nu_{1_0}, u_0))$ .

Then the solutions of  $F(\nu_1, u) = 0$  near  $(\nu_{1_0}, u_0)$  consist precisely of the curves  $u = u_0$  and  $(\nu_1(s), u(s))$ ,  $s \in I = (-\delta, \delta)$ , where  $(\nu_1(s), u(s))$  are continuously differentiable functions such that  $\nu_1(0) = \nu_{1_0}$ ,  $u(0) = u_0$ ,  $u'(0) = w_0$ . Moreover

$$\nu_1'(0) = -\frac{\langle l, F_{uu}(\nu_{1_0}, u_0)[w_0, w_0] \rangle}{2\langle l, F_{\nu_1 u}(\nu_{1_0}, u_0)[w_0] \rangle}, \quad (3.23)$$

where  $l \in \mathbf{R}^n$  satisfies  $R(F_u(\nu_{1_0}, u_0)) = \{y \in \mathbf{R}^n : \langle l, y \rangle = 0\}$ .

For our problem, we consider  $u = (U, V, W) \in \mathbf{R}^3$  and define

$$F(\nu_1, U, V, W) = \begin{pmatrix} U\phi(U) - a_1(U)UV - a_2(U, V)UW \\ \frac{\nu_1 W}{1 + \nu_2 W} + b_1 a_1(U)UV - \mu_1 V - b_2 a_2(U, V)VW \\ \epsilon V - \mu_2 W + b_3 a_2(U, V)UW + b_4 a_2(U, V)VW \end{pmatrix}. \quad (3.24)$$

We consider the bifurcation at  $(\nu_1, U, V, W) = (\nu_1^*, \kappa, 0, 0)$ . The linearized operator  $F_u(\nu_1^*, \kappa, 0, 0)$  is given by the Jacobian  $J(\kappa, 0, 0)$  defined in (3.18).

To find our eigenvector  $w_0 = (x, y, z)$  for  $J(\kappa, 0, 0)$  with zero eigenvalue, we solve the equation:

$$\begin{aligned} \kappa\phi'(\kappa)x - a_1(\kappa)\kappa y - a_2(\kappa, 0)\kappa z &= 0, \\ (b_1 a_1(\kappa)\kappa - \mu_1)y + \nu_1^* z &= 0, \\ \epsilon y + (-\mu_2 + b_3 a_2(\kappa, 0))z &= 0. \end{aligned} \quad (3.25)$$

The eigenvector for the zero eigenvalue can be written as follows:

$$w_0 = \begin{pmatrix} -\kappa[a_1(\kappa)\mu_2 - a_2(\kappa, 0)a_1(\kappa)b_3\kappa + a_2(\kappa, 0)\epsilon] \\ \mu_2 - b_3a_2(\kappa, 0)\kappa \\ \epsilon \end{pmatrix}. \quad (3.26)$$

Our range space is  $R = \{(x, y, z) \in \mathbf{R}^3 : \epsilon y = (-\mu_1 + b_1a_1(\kappa)\kappa)z\}$ . Thus, we have  $l = (0, \epsilon, \mu_1 - b_1a_1(\kappa)\kappa)$ .

For the denominator, we find:

$$F_{\nu_1 u}(\nu_{10}, u_0) = \begin{pmatrix} 0 & 0 & 0 \\ 0 & 0 & 1 \\ 0 & 0 & 0 \end{pmatrix}. \quad (3.27)$$

Thus, we have a simple calculation to determine that  $2\langle l, F_{\nu_1 u}(\nu_{10}, u_0)[w_0] \rangle = 2\epsilon^2$  for the general equation. It is tedious to find the numerator for the general case, so we will discuss this in each of the next two sections with the Lotka-Volterra case and the Holling Type II case.

## 3.2 Lotka-Volterra Case

In the Lotka-Volterra case, we have linear predation terms, rather than Holling Type II functional responses. Thus, our simpler version of the model is:

$$\begin{aligned} \frac{dU}{ds} &= U \left( 1 - \frac{U}{\kappa} \right) - a_1UV - a_2UW, \\ \frac{dV}{ds} &= \frac{\nu_1 W}{1 + \nu_2 W} + b_1a_1UV - \mu_1V - b_2a_2VW, \\ \frac{dW}{ds} &= \epsilon V - \mu_2W + b_3a_2UW + b_4a_2VW. \end{aligned} \quad (3.28)$$

Besides the parameter values given in Table 2.3, the new parameter values converted from Table 2.2 and 2.3 are:

	<i>Value</i>
$a_1$	.04
$a_2$	0.0288
$b_1$	50
$b_2$	1
$b_3$	1,000
$b_4$	0.2

Table 3.1: General Parameters

We have the trivial equilibria  $(0, 0, 0)$  and  $(\kappa, 0, 0)$  again. To consider the equilibrium  $(0, V^*, W^*)$ , we can take  $U = 0$  and study the two-dimensional system for  $V$  and  $W$ , which is:

$$\begin{aligned}\frac{dV}{ds} &= \frac{\nu_1 W}{1 + \nu_2 W} - \mu_1 V - b_2 a_2 V W, \\ \frac{dW}{ds} &= \epsilon V - \mu_2 W + b_4 a_2 V W.\end{aligned}\tag{3.29}$$

Setting  $V'$  and  $W'$  equal to 0 and solving for  $V$  in the second equation, we get  $V = \frac{\mu_2 W}{\epsilon + b_4 a_2 W}$ . From here, we plug  $V$  back into the first equation to get:

$$h_1(W) = \nu_1(\epsilon + b_4 a_2 W) - \mu_2(\nu_2 W + 1)(b_2 a_2 W + \mu_1) = 0.\tag{3.30}$$

We need to have  $h_1(0) < 0$  to ensure  $(0, V^*, W^*)$  exists. Thus, we need  $\mu_2 \mu_1 - \nu_1 \epsilon < 0$  for this to happen, which gives us again  $\nu_1 > \frac{\mu_1 \mu_2}{\epsilon} = \nu_1^\#$ . Hence a  $(0, V^*, W^*)$  type equilibrium exists whenever  $\nu_1 > \nu_1^\#$ .

We use `Matcont`, which is a numerical package for bifurcation analysis, to generate a bifurcation diagram. The bifurcation points in the diagram are marked with *BP*. *H* signifies a neutral saddle point, which we do not discuss here. These markings are described in such a manner in later bifurcation diagrams as well. In this bifurcation diagram (see Fig. 3.1), as  $\nu_1$  increases, initially we have the stable  $(\kappa, 0, 0)$  equilibrium; at

$\nu_1 = \nu_1^\#$ , the  $(U^*, V^*, W^*)$  equilibrium bifurcates from the line of  $(\kappa, 0, 0)$  equilibria and becomes stable. Lastly at some larger  $\nu_1$  value, the  $(0, V^*, W^*)$  equilibrium becomes the stable one.

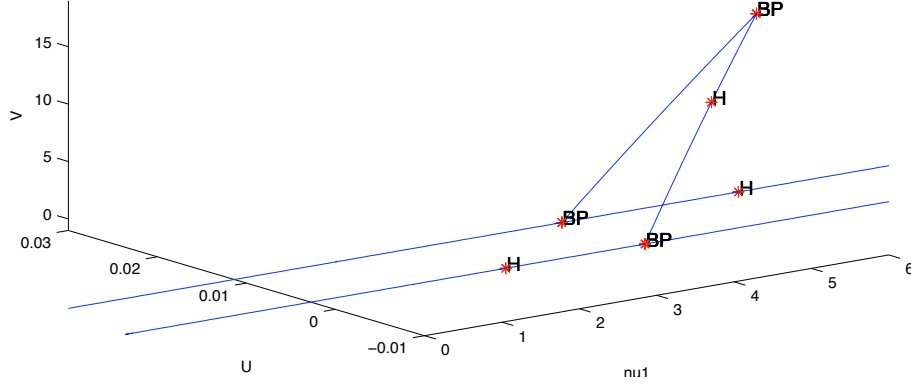


Figure 3.1: Bifurcation Diagram of Lotka-Volterra Case (3.28)

Parameters used from Tables 2.3 and 3.1, allowing  $\nu_1$  to vary.

### 3.2.1 Lotka-Volterra Bifurcation Derivative

In the previous section, we determined that we can find  $\nu_1'(0)$  by using Theorem 3.1, which states:

$$\nu_1'(0) = -\frac{\langle l, F_{uu}(\nu_{1_0}, u_0)[w_0, w_0] \rangle}{2\langle l, F_{\nu_1 u}(\nu_{1_0}, u_0)[w_0] \rangle}. \quad (3.31)$$

We know that the denominator is  $2\epsilon^2$ , so now we calculate the numerator where  $F_{uu} = (K_{ijk})_{i,j,k} = (\partial_{jk} F_i)_{i,j,k}$  where  $\partial_{jk} F_i = \frac{\partial^2 F_i(\nu_1, u)}{\partial u_j \partial u_k}$ . Thus, for our case, we have:

$$F_{uu}[(x_1, x_2, x_3), (y_1, y_2, y_3)] = \left( \sum_{j,k=1}^3 K_{1jk} x_j y_k, \sum_{j,k=1}^3 K_{2jk} x_j y_k, \sum_{j,k=1}^3 K_{3jk} x_j y_k \right). \quad (3.32)$$

Also, we use  $l$  and  $w_0$  as defined earlier. Here, we define  $\phi_1 = \mu_1 - b_1 a_1 \kappa$ ,  $\phi_2 = \mu_2 - b_3 a_2 \kappa$ , and  $\phi_3 = -\kappa[a_1 \mu_2 - a_1 a_2 b_3 \kappa + a_2 \epsilon] = -\kappa[a_1 \phi_2 + a_2 \epsilon]$  for convenience.



Now we calculate  $K_{ijk}$ , use (3.32), and substitute  $\nu_1^* = \frac{\phi_1\phi_2}{\epsilon}$  and reduce to get:

$$\nu_1'(0) = \frac{1}{\epsilon}[\phi_2\epsilon(a_2b_2 + \nu_2\phi_1) + a_2\kappa(b_1\phi_2 + b_3\phi_1)(a_1\phi_2 + a_2\epsilon) - a_2b_4\phi_1\phi_2]. \quad (3.33)$$

In our attempt to make  $\nu_1'(0) < 0$ , to determine what is necessary for the system to show evidence of bistability, we can increase  $b_4$  or decrease both  $b_2$  and  $\nu_2$ , since we know all parameters in (3.33) are positive. From here, we determine a critical  $\nu_2^*$  to be as follows:

$$\nu_2^* = \frac{a_2[b_4\phi_1\phi_2 - \kappa(b_1\phi_2 + b_3\phi_1)(a_1\phi_2 + a_2\epsilon) - b_2\phi_2\epsilon]}{\phi_1\phi_2\epsilon}. \quad (3.34)$$

When  $\nu_2 < \nu_2^*$ , we will have  $\nu_1'(0) < 0$ . A possible bifurcation diagram generated by `Matcont` is shown in Fig. 3.2. Here, we see the potential for bistability due to the negative slope of the bifurcation from  $(\kappa, 0, 0)$ .

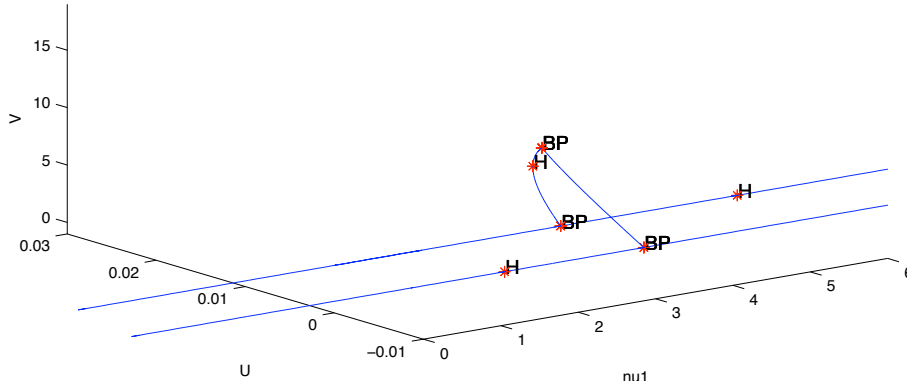


Figure 3.2: Bifurcation Diagram with Bistability of Lotka-Volterra Case (3.28)  
Parameters used from Tables 2.3 and 3.1, except  $b_4 = 6$ , allowing  $\nu_1$  to vary.

### 3.3 Holling Type II Case

Using Holling Type II Functional responses, our model is now:

$$\begin{aligned}
\frac{dU}{ds} &= U \left( 1 - \frac{U}{\kappa} \right) - \frac{a_1 UV}{U+1} - \frac{a_2 UW}{\theta U + \delta \psi V + 1}, \\
\frac{dV}{ds} &= \frac{\nu_1 W}{1 + \nu_2 W} + \frac{b_1 a_1 UV}{U+1} - \mu_1 V - \frac{b_2 a_2 VW}{\theta U + \delta \psi V + 1}, \\
\frac{dW}{ds} &= \epsilon V - \mu_2 W + \frac{b_3 a_2 UW + b_4 a_2 VW}{\theta U + \delta \psi V + 1}.
\end{aligned} \tag{3.35}$$

Figure 3.3 is our bifurcation diagram for the Holling Type II case. Similarly to the Lotka-Volterra model, we have a stable branch of  $(\kappa, 0, 0)$  when  $\nu_1 < \nu_1^*$ , then the coexistence equilibrium  $(U^*, V^*, W^*)$  is stable when  $\nu_1^* < \nu_1 < \tilde{\nu}_1$  for  $\tilde{\nu}_1$  another bifurcation parameter which will be discussed later. We also have the  $(0, V^*, W^*)$  equilibrium which bifurcates from the trivial equilibrium at  $\nu_1 = \nu_1^\#$  and then becomes stable at a larger  $\nu_1$  value.

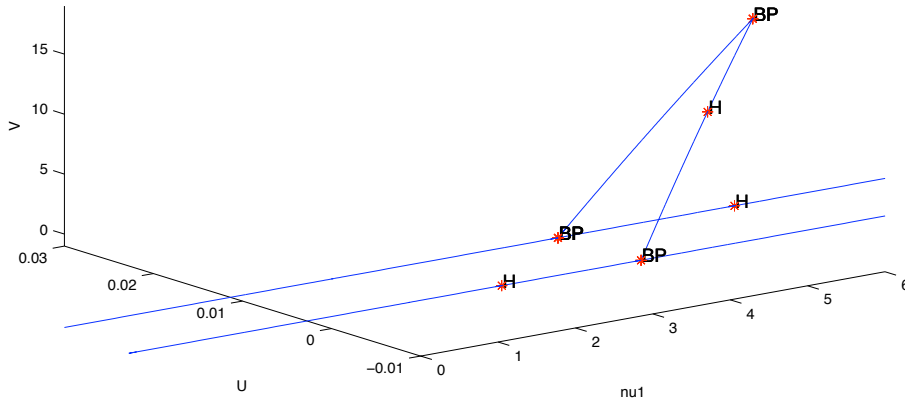


Figure 3.3: Bifurcation Diagram of (3.35)

Parameters used from Tables 2.3 and 3.1, allowing  $\nu_1$  to vary.

### 3.3.1 Holling Type II Bifurcation Derivative

Similarly to the Lotka-Volterra case, we have the bifurcation derivative as follows:

$$\nu_1'(0) = -\frac{\langle l, F_{uu}(\nu_{10}, u_0)[w_0, w_0] \rangle}{2\langle l, F_{\nu_1 u}(\nu_{10}, u_0)[w_0] \rangle}. \quad (3.36)$$

We know that the denominator is  $2\epsilon^2$ . We can calculate the numerator similar to the Lotka-Volterra case, where  $l$  and  $w_0$  are as defined earlier. Again we define

$$\begin{aligned} \phi_1 &= \mu_1 - b_1 a_1(\kappa) \kappa = \mu_1 - \frac{b_1 a_1 \kappa}{\kappa + 1}, \\ \phi_2 &= \mu_2 - b_3 a_2(\kappa, 0) \kappa = \mu_2 - \frac{b_3 a_2 \kappa}{\kappa \theta + 1}, \end{aligned}$$

and

$$\phi_3 = -\kappa [a_1(\kappa) \mu_2 - a_2(\kappa, 0) a_1(\kappa) b_3 \kappa + a_2(\kappa, 0) \epsilon] = -\kappa \left[ \frac{a_1 \phi_2}{\kappa + 1} + \frac{a_2 \epsilon}{\kappa \theta + 1} \right]$$

for convenience. Additionally, we substitute in  $\nu_1^* = \frac{\phi_1 \phi_2}{\epsilon}$ . Thus, we have:

$$\begin{aligned} \nu_1'(0) &= \frac{1}{\epsilon} \left[ \frac{a_2 b_2 \phi_2}{(\kappa \theta + 1)^2} (\epsilon + a_2 b_3 \kappa \psi \phi_1) + \nu_2 \phi_1 \phi_2 \epsilon \right. \\ &\quad \left. + \kappa \left( \frac{a_1 \phi_2}{\kappa \theta + 1} + \frac{a_2 \epsilon}{(\kappa \theta + 1)^2} \right) \left( \frac{a_1 b_1 \phi_2}{(\kappa + 1)^2} + \frac{a_2 b_3 \phi_1}{(\kappa \theta + 1)^2} \right) - \frac{a_2 b_4 \phi_1 \phi_2}{\kappa \theta + 1} \right]. \end{aligned} \quad (3.37)$$

Again we can use  $b_2, b_4$  or  $\nu_2$  as our switching parameters. To make  $\nu_1'(0) < 0$ , we can decrease  $b_2$  and  $\nu_2$ , or increase  $b_4$ . For example, we can determine a  $\nu_2^*$  as the point at which the sign of the derivative changes:

$$\nu_2^* = \frac{M}{\phi_1 \phi_2 \epsilon}, \quad (3.38)$$

where

$$\begin{aligned} M &= \frac{a_2 b_4 \phi_1 \phi_2}{\kappa \theta + 1} - \frac{a_2 b_2 \phi_2}{(\kappa \theta + 1)^2} (\epsilon + a_2 b_3 \kappa \psi \phi_1) \\ &\quad - \kappa \left( \frac{a_1 \phi_2}{\kappa \theta + 1} + \frac{a_2 \epsilon}{(\kappa \theta + 1)^2} \right) \left( \frac{a_1 b_1 \phi_2}{(\kappa + 1)^2} + \frac{a_2 b_3 \phi_1}{(\kappa \theta + 1)^2} \right). \end{aligned} \quad (3.39)$$

Figure 3.4 is a potential bifurcation diagram with bistability, wherein the slope of our bifurcation derivative at  $(\kappa, 0, 0)$  is negative. These specific parameters give evidence of bistability in (3.35).

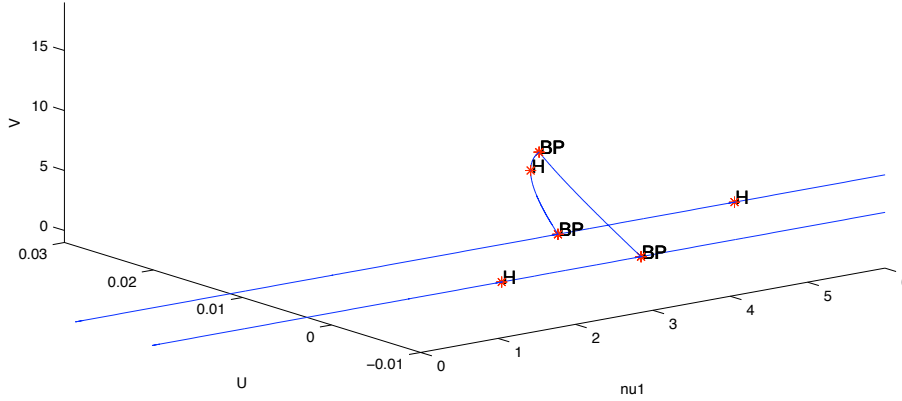


Figure 3.4: Bifurcation Diagram with Bistability of (3.35)

Parameters used from Tables 2.3 and 3.1, except  $\gamma_4 = 6$ , allowing  $\nu_1$  to vary.

### 3.4 Numerical Simulations

Using `Matlab`, we draw time-series diagrams to have a sense of the change of the dynamical behavior. In both models, we have:

$$\begin{aligned}
 \nu_1 < \nu_1^* &\rightarrow (\kappa, 0, 0) \text{ is stable,} \\
 \nu_1^* < \nu_1 < \tilde{\nu}_1 &\rightarrow (U^*, V^*, W^*) \text{ is stable,} \\
 \tilde{\nu}_1 < \nu_1 &\rightarrow (0, V^*, W^*) \text{ is stable.}
 \end{aligned}
 \tag{3.40}$$

The bifurcation point,  $\tilde{\nu}_1$ , was only found numerically. It is the point at which the  $(0, V^*, W^*)$  equilibrium becomes stable. This is an unphysical due to the fact that  $(0, V^*, W^*)$  is an unphysical equilibrium that becomes stable here. Additionally, it is unphysical since  $\tilde{\nu}_1$  suggests that the birth rate of  $\nu_1$  is greater than what should be physically possible in nature. The reason for the stability even with the loss of the resource is due to the birth rate being so high that it outpaces the death terms. Thus, we have found this equilibrium to be stable using `Matcont` and `Matlab`, but it is not something

that is possible to see in nature.

We can plot time series of solutions and analyze their graphs as well. In Fig. 3.5, 3.6 and 3.7, the three scenarios described above are simulated.

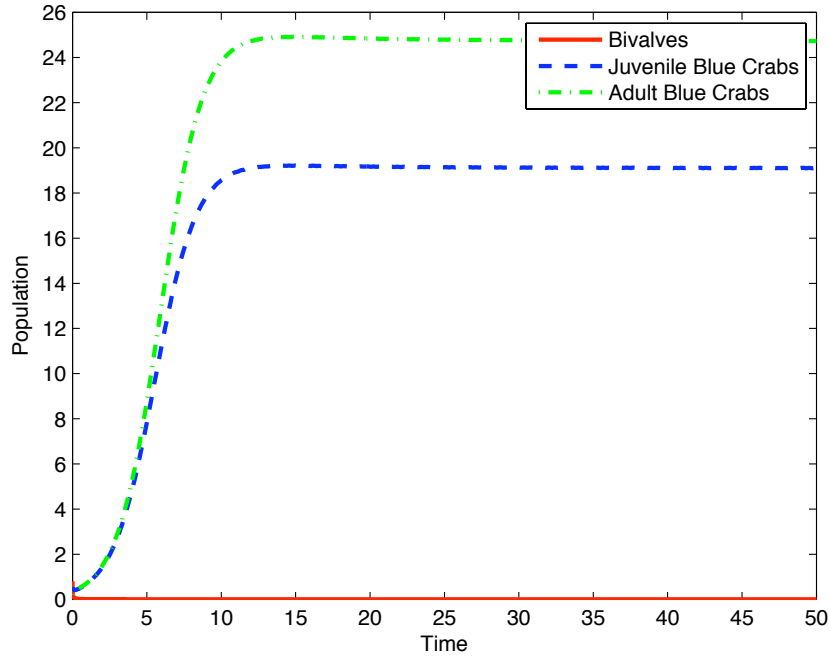


Figure 3.5: Extinction of Resource:  $\nu_1 > \tilde{\nu}_1$ . The solution approaches  $(0, V^*, W^*)$   
Parameters used:  $\gamma_1 = 0.04$ ,  $\lambda = 0.0288$ ,  $\theta = 1.44$ ,  $\psi = 0.01$ ,  $\kappa = 0.02$ ,  $\nu_2 = 0.01$ ,  $\gamma_2 = 2$ ,  
 $\delta = 0.0288$ ,  $\mu_1 = 5$ ,  $\epsilon = 4$ ,  $\gamma_3 = 28.8$ ,  $\mu_2 = 3.2$ ,  $\gamma_4 = 0.2$ .  
Initial value:  $(U, V, W) = (0.8, 0.5, 0.2)$ . Our bifurcation values are  $\nu_1^* = 3.917$ ,  $\nu_1^\# = 4$ ,  
and  $\tilde{\nu}_1 = 5.444$ .  
Here,  $\nu_1 = 5.5$ , extinction of resource.

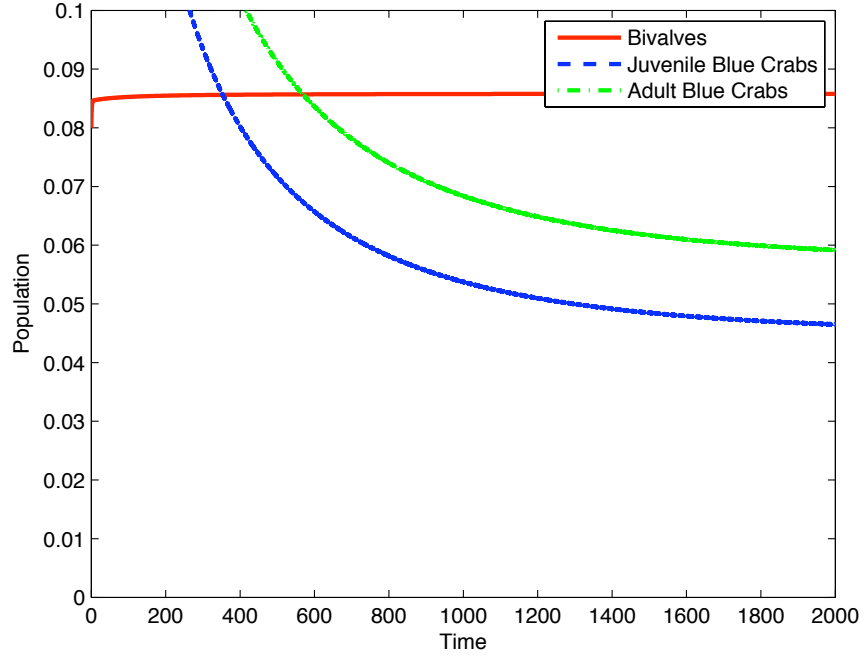


Figure 3.6: Persistence of Blue Crab:  $\nu_1^* < \nu_1 < \tilde{\nu}_1$ . The solution approaches  $(U^*, V^*, W^*)$

Parameters used:  $\gamma_1 = 0.04$ ,  $\lambda = 0.0288$ ,  $\theta = 1.44$ ,  $\psi = 0.01$ ,  $\kappa = 0.02$ ,  $\nu_2 = 0.01$ ,  $\gamma_2 = 2$ ,  
 $\delta = 0.0288$ ,  $\mu_1 = 5$ ,  $\epsilon = 4$ ,  $\gamma_3 = 28.8$ ,  $\mu_2 = 3.2$ ,  $\gamma_4 = 0.2$ .

Initial value:  $(U, V, W) = (0.008, 0.3, 0.4)$ . Our bifurcation values are  $\nu_1^* = 3.917$ ,

$$\nu_1^\# = 4, \text{ and } \tilde{\nu}_1 = 5.444.$$

Here,  $\nu_1 = 3.92$ , persistence of blue crab.

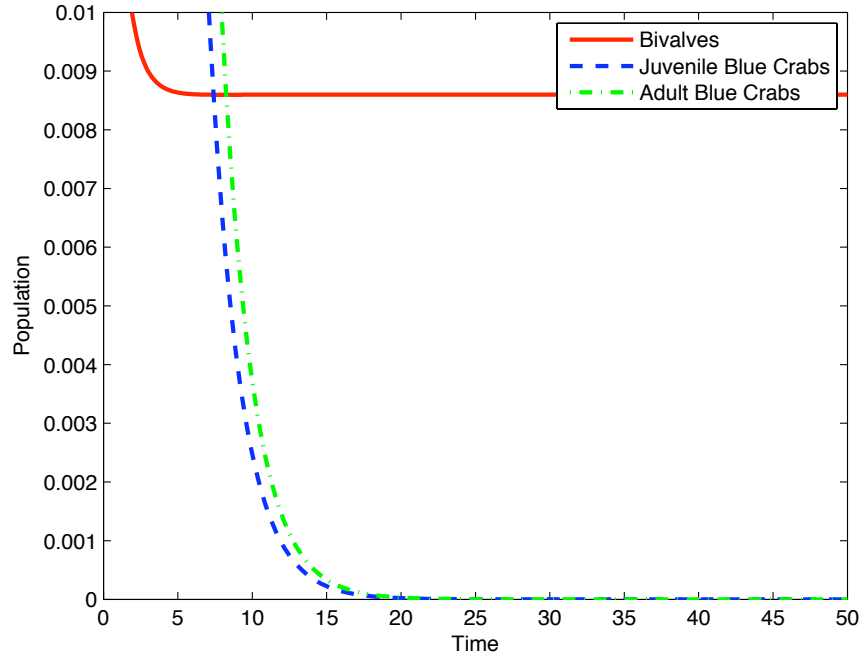


Figure 3.7: Extinction of Blue Crab:  $\nu_1 < \nu_1^*$ . The solution approaches  $(\kappa, 0, 0)$   
Parameters used:  $\gamma_1 = 0.04$ ,  $\lambda = 0.0288$ ,  $\theta = 1.44$ ,  $\psi = 0.01$ ,  $\kappa = 0.02$ ,  $\nu_2 = 0.01$ ,  $\gamma_2 = 2$ ,  
 $\delta = 0.0288$ ,  $\mu_1 = 5$ ,  $\epsilon = 4$ ,  $\gamma_3 = 28.8$ ,  $\mu_2 = 3.2$ ,  $\gamma_4 = 0.2$ .  
Initial value:  $(U, V, W) = (0.8, 0.5, 0.2)$ . Our bifurcation values are  $\nu_1^* = 3.917$ ,  $\nu_1^\# = 4$ ,  
and  $\tilde{\nu}_1 = 5.444$ .  
Here,  $\nu_1 = 3.8$ , extinction of blue crab.



### 3.4.1 Matlab Code for Numerical Simulations

```
function bluecrabbiomass

%parameters
%intervals of time which to run the model
tspan=[0 50];
%the initial condition for the bivalves, juveniles, and adults
y0=[0.8; 0.5; 0.2];
kappa=0.0086;
gamma1=0.0172;
lambda=0.0288;
psi=0.01;
nu1=3;
nu2=0.01;
gamma2=2;
theta=3.3488;
mu1=5;
delta=0.0288;
epsilon=4;
gamma3=6.6977;
mu2=3.2;
gamma4=0.2;

[T,Y]=ode45(@f,tspan,y0);
%subplot(4,1,3)
plot(T,Y(:,1),'-r',T,Y(:,2),'--b',T,Y(:,3),'-.g','linewidth',2);
```

```

axis([0 50 0 14])
set(gca,'YTick',[0 1 2 3 4 5 6 7 8 9 10 11 12 13 14])
%set(gcf,'DefaultAxesColorOrder',[1 0 0;0 1 0;0 0 1])
%plot(T,Y);
xlabel('Time');
ylabel('Population');
legend('Bivalves', 'Juvenile Blue Crabs', 'Adult Blue Crabs')

function dy=f(t,y)

dy = zeros(3,1);    % a column vector

dy(1) = y(1)*(1-y(1)/kappa)-(gamma1*y(1)*y(2))/(y(1)+1)
-(lambda*y(1)*y(3))/(theta*y(1)+delta*psi*y(2)+1);
dy(2) = (nu1*y(3))/(1+nu2*y(3))+(gamma2*y(1)*y(2))/(y(1)+1)
-mu1*y(2)-(delta*y(2)*y(3))/(theta*y(1)+delta*psi*y(2)+1);
dy(3) = epsilon*y(2)-mu2*y(3)+(gamma3*y(1)*y(3)
+delta*gamma4*y(2)*y(3))/(theta*y(1)+delta*psi*y(2)+1);
end
end

```

# Chapter 4

## Conclusions

The blue crab is important to both the Chesapeake Bay ecosystem, as well as the economy of the area. Due to this, the decrease in population levels of the crab must be addressed. This model is constructed with the purpose of helping the Virginia Institute of Marine Science in their efforts to bring the blue crab population up to historic levels. The blue crab partakes in both intraguild predation and cannibalism, so both of these aspects must be stressed in the model.

We developed our new model based on previous intraguild predation models, especially Verdy and Amarasekere's model from 2009 [20]. We introduced one additional feedback mechanism into their model. This is our cannibalism term. Additionally, we introduce an aging term into the model to describe the growth from the juvenile class into the adult class. We used a Beverton-Holt birth term and also a linear harvesting rate of the adult blue crab. We used both a Lotka-Volterra model and a Holling Type II model to work with a simplified model as well as a model that accurately represented the functional responses of the crabs as well as the bivalves. Thus, we determined our model for the blue crab.

We analyzed the general model for biologically reasonable parameters and found that we have the trivial equilibrium  $(0, 0, 0)$ , as well as the semi-trivial equilibria  $(\kappa, 0, 0)$  and

$(0, V^*, W^*)$ . Lastly, we have the coexistence equilibrium  $(U^*, V^*, W^*)$ . The trivial equilibrium is always unstable, while the others are stable or unstable depending on the choice of parameters.  $(\kappa, 0, 0)$  is the extinction equilibrium, in which the juvenile and adult blue crabs go extinct and the bivalves go to the carrying capacity,  $\kappa$ . It is stable for a low birthing rate of blue crabs, which we defined as our bifurcation parameter.  $(U^*, V^*, W^*)$  is the coexistence equilibrium, where the juvenile and adult blue crabs persist, as well as the bivalves. This equilibrium is stable after it bifurcates from the  $(\kappa, 0, 0)$  equilibrium. Lastly, we have the extinction of resource equilibrium  $(0, V^*, W^*)$ , which describes the extinction of the bivalve, but the persistence of the juvenile and adult blue crab based on cannibalism. This equilibrium is stable for some biologically non-reasonable birthing rate. Mathematically, however, we do find this equilibrium.

We simulate the model using `Matlab`, specifically `ode45`. These numerical simulations demonstrated again the three stable equilibria depending on the initial parameter value for the birthing rate. Additionally, we use `Matcont` to determine the presence of bistability in both the Lotka-Volterra and Holling Type II cases, using the calculations from the bifurcation theorem.

We hope that this work will help the Virginia Institute of Marine Science researchers in their work with the blue crab in the Chesapeake Bay. Our model will help VIMS understand the dynamics of the blue crab, including but not limited to the cannibalism in the blue crab. With this knowledge, we believe that VIMS will be able to make steps forward in their own blue crab research and conservation.

In the future, we will study the parameter estimates again, as mentioned in Section 1.4 and work to obtain more accurate estimates. This will be used to further analyze and study the model, as well as leading to new numerical simulations.

## 4.1 Acknowledgements

This research is supported by William and Mary Charles Center Honors Fellowship and NSF CSUMS grant. Thank you to the best three advisors I could have possibly had. Firstly, thank you to Professor Junping Shi for approaching me to work on this project and for his constant willingness to help me at any time. Thank you to Professor Rom Lipcius for everything he taught me about the blue crab and his contagious enthusiasm for the project. Lastly, thank you to Professor Leah Shaw for answering all of my questions and helping me to understand the necessary mathematical biology for the project.



# Bibliography

- [1] Abrams, P., Fung, S. Prey persistence and abundance in systems with intraguild predation and type-2 functional responses. *Jour. Theo. Biol.* 264 (2010), 1033–1042.
- [2] Amarasekare, P. Productivity, dispersal, and the coexistence of intraguild predators and prey. *Jour. Theo. Biol.* 243 (2006), 121–133.
- [3] Amarasekare, P. Trade-offs, temporal variation, and species coexistence in communities with intraguild predation. *Ecology* 88 (2007), 2720–2728.
- [4] Amarasekare, P. Coexistence of intraguild predators and prey in resource-rich environments. *Ecology* 89 (2008), 2786–2797.
- [5] Britton, N. F. “Essential Mathematical Biology.” Springer Verlag London Limited; 2003.
- [6] Brown, J. H. Towards a metabolic theory of ecology. *Ecology* 85 (2004), 1771–1789.
- [7] Crandall, Michael G.; Rabinowitz, Paul H. Bifurcation from simple eigenvalues. *J. Functional Analysis*, 8 (1971), 321–340.
- [8] Cushing, J. M. A simple model of cannibalism. *Math. Biosci.* 107 (1991), 47–71.
- [9] Eggleston, D.B. Functional responses of blue crabs *Callinectes sapidus* Rathbun feeding on juvenile oysters *Crassostrea virginica* (Gmelin): effects of predator sex and size, and prey size. *J. Exp. Mar. Biol. Ecol.* 143 (1990), 73–90.

- [10] Eggleston, D.B.; Lipcius, R.N.; Hines, A.H. Density-dependent predation by blue crabs upon infaunal clam species with contrasting distribution and abundance patterns. *Mar. Ecol. Prog. Ser.* 85 (1992), 55–68.
- [11] Holt, R. D.; Polis, G. A. A theoretical framework for intraguild predation. *Am. Nat.* 149 (1997), 745–764.
- [12] Lotka, A.J. “Elements of Mathematical Biology.” Dover Publications; New York. 1956.
- [13] Kennedy, V., Cronin L. “The Blue Crab: *Callinectes sapidus*.” Maryland Sea Grant College; College Park, Maryland. 2007.
- [14] Kleiber, M. Body size and metabolism. *Hilgardia* 6 (1932), 315–332.
- [15] McCann, K., Hastings, A., Re-evaluating the omnivory, stability relationship in food webs. *Proc. R. Soc. B* 264 (1997), 1249–1254.
- [16] Polis, G., Myers, C., Holt, R. The Ecology and Evolution of Intraguild Predation. *Annual Review of Ecology and Semantics* 20 (1989), 297–330.
- [17] Real, Leslie A. The Kinetics of Functional Reponse. *The American Naturalist* 111 (1977), 289–300.
- [18] Romuald Lipcius, Virginia Institute of Marine Science–Personal Communication. 2012.
- [19] Stock Assessment of the Blue Crab in the Chesapeake Bay 2011. University of Maryland Center for Environmental Science. 2011.
- [20] Verdy, A.; Amarasekare, P. Alternative stable states in communities with intraguild predation. *Jour. Theo. Biol.* 262 (2010), 116–128.



- [21] Volterra, V. Fluctuations in the Abundance of a Species Considered Mathematically. *Nature* 118 (1926) 558-560.